Supplementary Information

Conjugated polymer nanoparticles based on anthracene and tetraphenylethene for nitroaromatics detection in aqueous phase

Tianwen Ouyang[a], Xue Guo[a], Qihao Cui[a], Wei Zhang[a], Wenyue Dong[a,*], Teng Fei[b,*]

[a] School of Materials Science and Engineering, Changchun University of Science and Technology, Changchun, 130022, PR China

[b] State Key Laboratory of Integrated Optoelectronics, College of Electronic Science and Engineering, Jilin University, Changchun, 130012, PR China

*Corresponding author:

dongwenyue@cust.edu.cn (W. Dong)

feiteng@jlu.edu.cn (T. Fei)

Content

Reagents and measurements

Zinc powder, sodium bicarbonate, sodium sulfate, potassium carbonate, magnesium sulfate and toluene were obtained from Beijing Chemical Works. Absolute ethanol, dichloromethane, tetrahydrofuran, petroleum ether was purchased from Tianjin Fuyu Fine Chemical Co. Sodium dodecyl sulfate, 4-bromobenzophenone, 4,4-dibromodibenzophenone were purchased from Energy Chemical. Titanium tetrachloride and Calcium hydride were obtained from Macklin and Aladdin. The experimental water was deionized water. Tetrahydrofuran/toluene were dried and purified by distillation over calcium hydride.

FT–IR spectra in KBr were performed on PerkinElmer Fourier transform infrared spectrometer. UV–Vis spectra were tested by UV-1240 UV–Vis spectrophotometer of SHIMADZU. The ^{1}H NMR and ^{13}C NMR spectra were characterized by AV-500 nuclear magnetic resonance instrument of Bruker. Fluorescence spectra were measured on the fluorescence spectrometer LS-55 of PerkinElmer. The nitrogen isothermal adsorption desorption curves were obtained on SSA-4000 aperture and specific surface area analyzer. The specific surface areas of the samples were calculated by Brunauer Emmett Teller (BET) method, and the pore diameters were calculated by Barrett–Joyner–Hallenda (BJH) method. Scanning electron microscope (SEM) images were measured by JEM-6701F scanning electron microscope of JEOL. Transmission electron microscope (TEM) images were measured by JEOL JEM-2100F transmission electron microscopy. Dynamic light scattering (DLS) experiments were carried out on a DynaPro NanoStar instrument (Wyatt Technology). The cyclic voltammetry (CV) curves were tested by 100 B/W of BAS electrochemical workstation. The initial oxidation potential E_{OX}^{onset} was determined according to the intersection of two tangents drawn at the rising current and background current in the CV curve. Fluorescence lifetimes were measured by Flou Time 300 automatic fluorescence lifetime spectrometer of Wuhan Donglong Technology Co., Ltd.

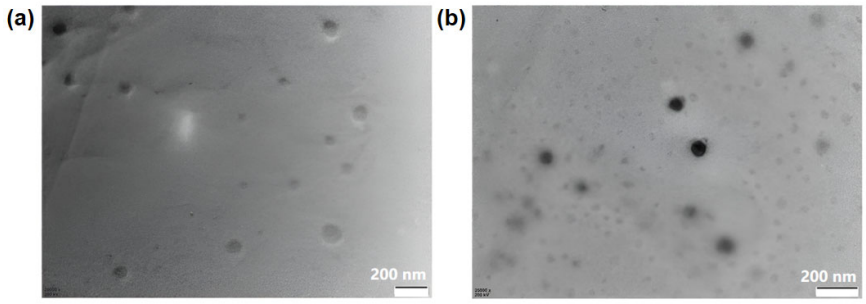

Figure S1. TEM images of *l*-PAnTPE (a) and PAnTPE (b).

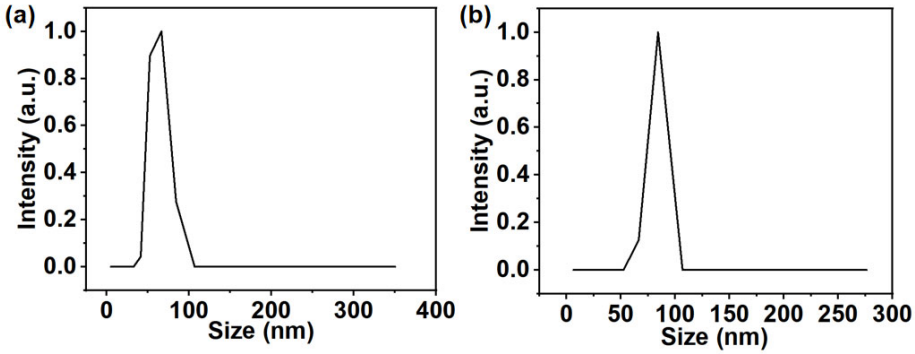

Figure S2. DLS curves of *l*-PAnTPE (a) and PAnTPE (b).

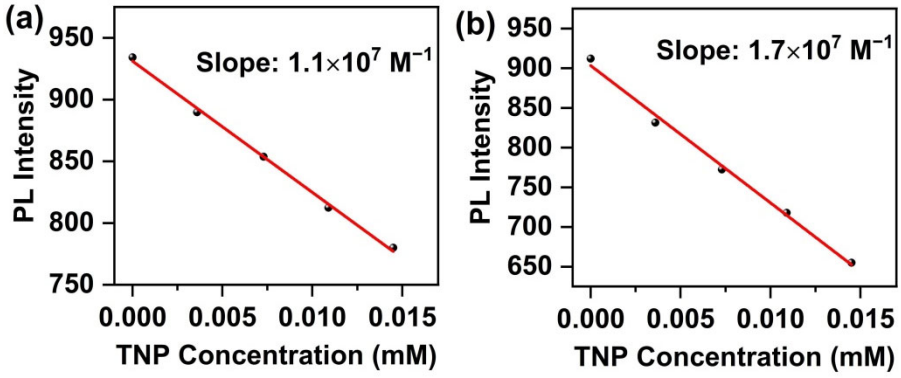

Figure S3. Linear relationship between different quantities of TNP and PL intensities of polymers *l*-PAnTPE (a) and PAnTPE (b) aqueous dispersion.

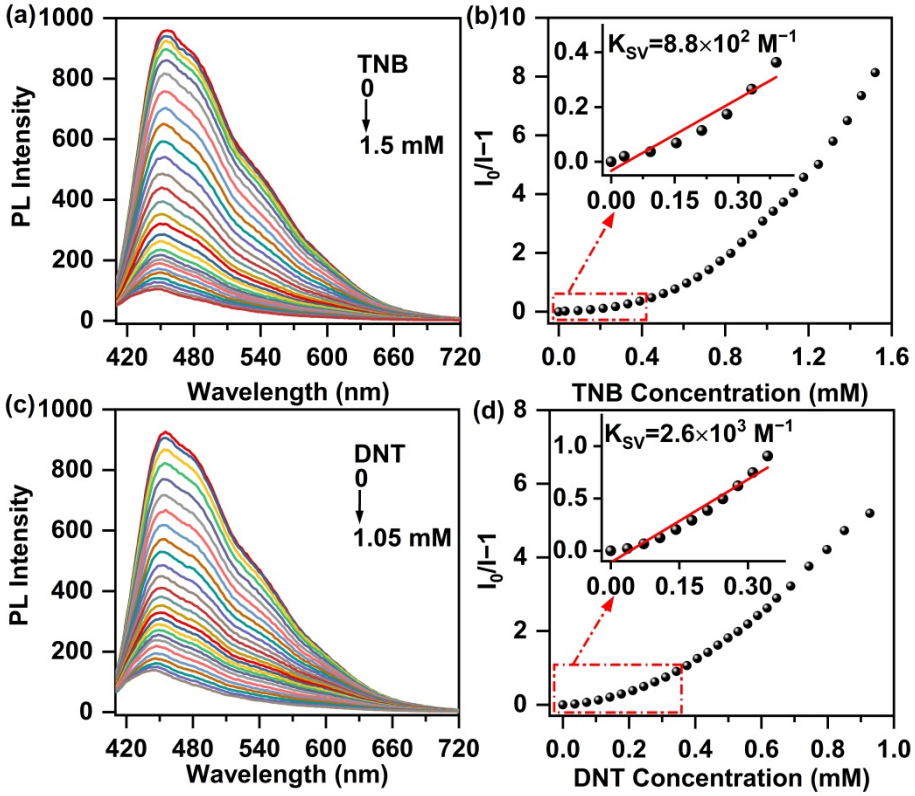

Figure S4. Emission spectra of *l*-PAnTPE aqueous dispersion by addition of TNB (a) and DNT (c). S–V plots of relative PL intensities ($I_0/I-1$) of *l*-PAnTPE vs. TNB (b) and DNT (d) concentration.

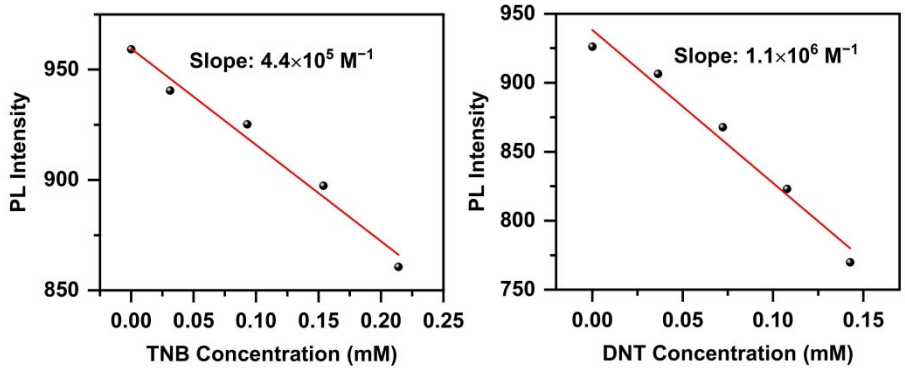

Figure S5. Linear relationship between different quantities of explosives and PL intensity of *l*-PAnTPE aqueous dispersion.

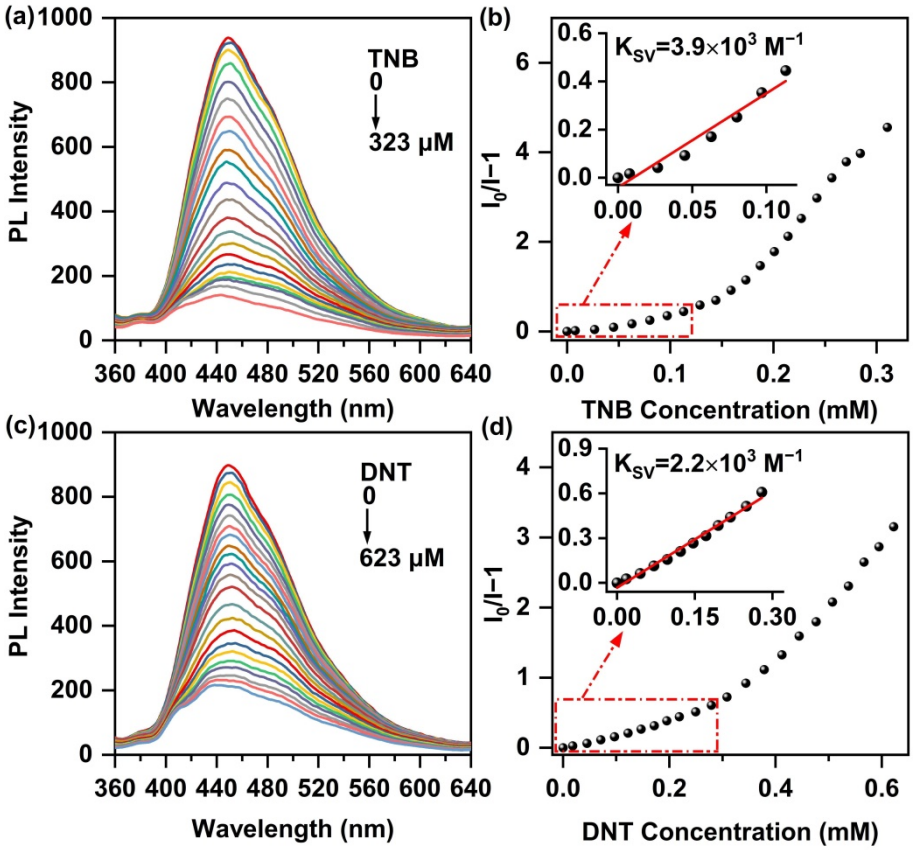

Figure S6. Emission spectra of PAnTPE aqueous dispersion by addition of TNB (a) and DNT (c). S–V plots of relative PL intensities ($I_0/I-1$) of PAnTPE vs. TNB (b) and DNT (d) concentration.

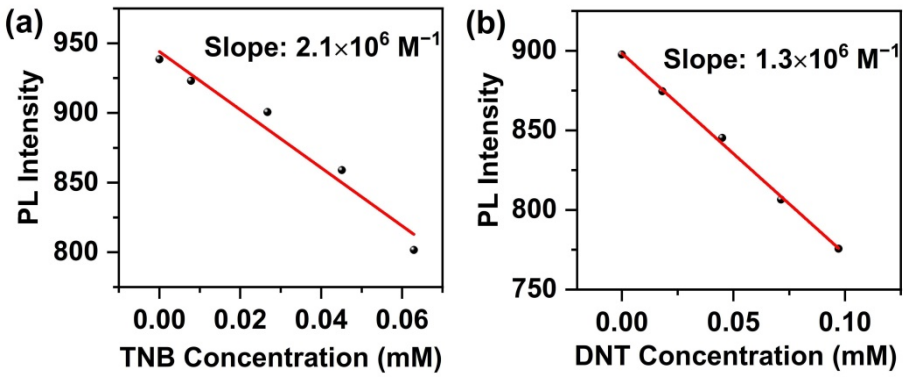

Figure S7. Linear relationship between different quantities of explosives and PL intensity of PAnTPE aqueous dispersion.

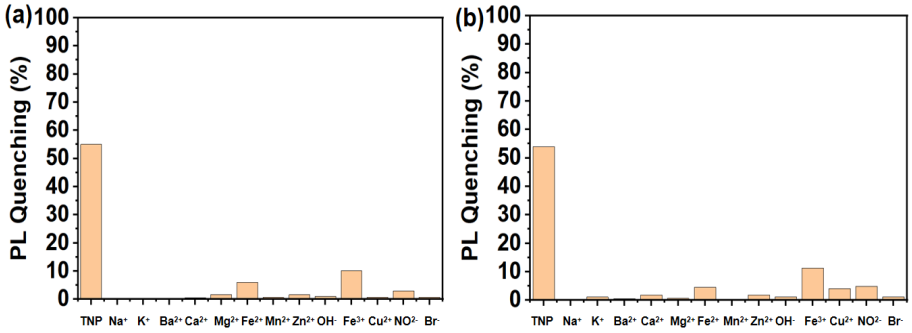

Figure S8. PL quenching degree of *l*-PAnTPE (a) and PAnTPE (b) aqueous dispersion by adding potential interfering ions (Na^+, K^+, Ba^{2+} and Ca^{2+} of 450 μM; Mg^{2+}, Fe^{2+}, Mn^{2+}, Zn^{2+} and OH^- of 200 μM; Fe^{3+}, Cu^{2+}, NO_2^- and Br^- of 100 μM) and TNP (70 and 35 μM in *l*-PAnTPE and PAnTPE, respectively).

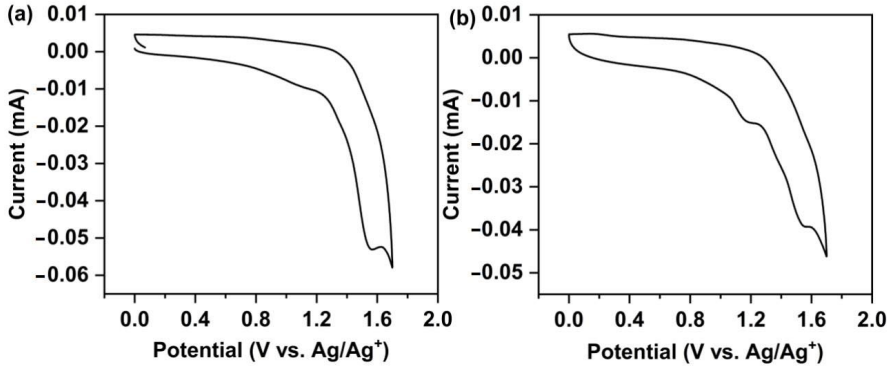

Figure S9. The cyclic voltammogram curves of *l*-PAnTPE (a) and PAnTPE (b) in acetonitrile.

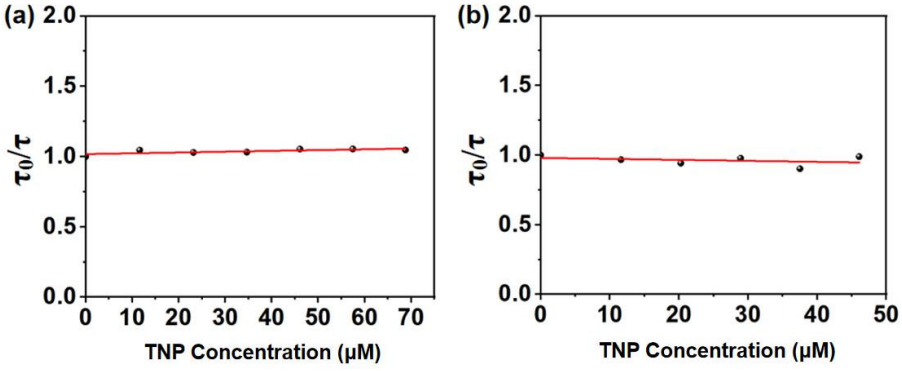

Figure S10. Linear fitting of τ_0/τ of *l*-PAnTPE (a) and PAnTPE (b) vs. TNP concentration, where τ_0 is the average PL lifetime of polymer dispersion, and τ is the average PL lifetime upon TNP addition.

Table S1. LODs and LOQs of *l*-PAnTPE for TNP, TNB and DNT, respectively.

	TNP	**TNB**	**DNT**
Standard deviation (б)	2.4302	2.4302	2.4302
Slope (K)	1.1×10^{7}	4.4×10^{5}	1.1×10^{6}
LOD	663 nM	16.6 μM	6.60 μM
LOQ	2.20 μM	55.2 μM	22.1 μM

Table S2. LODs and LOQs of PAnTPE for TNP, TNB and DNT, respectively.

	TNP	**TNB**	**DNT**
Standard deviation (б)	2.4875	2.4875	2.4875
Slope (K)	1.7×10^{7}	2.1×10^{5}	1.3×10^{6}
LOD	439 nM	3.60 μM	5.70 μM
LOQ	1.50 μM	11.8 μM	19.1 μM